swiss physical society

Nr. 57
März 2019

SPG MITTEILUNGEN
COMMUNICATIONS DE LA SSP

AUSZUG - EXTRAIT

Progress in Physics (66)

The attosecond science of solids

Lukas Gallmann and Ursula Keller, ETH Zürich

This article has been downloaded from:
https://www.sps.ch/fileadmin/articles-pdf/2019/Mitteilungen_Progress_66.pdf

© see https://www.sps.ch/bottom_menu/impressum/

Progress in Physics (66)

The attosecond science of solids

Lukas Gallmann and Ursula Keller, ETH Zürich

1. Introduction

The field of experimental attosecond science started in 2001 with the first successful characterization of attosecond extreme ultraviolet (XUV) bursts of radiation by two independent teams [1, 2]. Attosecond science is a sub-domain of ultrafast science that uses short laser pulses to time-resolve some of the fastest processes in nature. Given that the lightest and fastest nuclei vibrate with a 8 fs period in ground-state molecular hydrogen, it becomes evident that nuclear motion is essentially frozen on attosecond time scales. As a result, one may ask what kind of attosecond dynamics remains to be observed in this case? It is the motion of electrons, the lightest constituents of matter, that unfolds in this domain.

Due to the technical complexity of attosecond experiments, early studies concentrated on gas phase systems and, in particular, on rare gas atoms. These experiments helped to improve our understanding of the dynamics of light-induced ionization processes, ranging from single-photon ionization to tunnel ionization. In recent years, the field expanded to molecules, the liquid phase and solids.

Similar to the insights ever improving microscopy tools yielded on the structure of matter, attosecond science provides a close-up view of ultrafast dynamics in the time domain. Processes that can be approximated as instantaneous in other regimes have to be revisited and theoretical models have to be refined accordingly. New questions can be asked that were previously inaccessible to experimental studies. How long does it take for an electron to tunnel through a classically forbidden barrier? How long does it take to photoemit an electron from an atom, molecule or solid surface? How do the electrons in a solid transiently respond to an ultrafast – potentially THz to PHz – modulation through an applied electric field? While the former questions are of a fundamental nature, the latter also has direct consequences for the ultimate limits to electronic device performance.

In the following, we will review the state of attosecond science of solid systems. We illustrate its capabilities based on our recent work on optical-field-driven electron dynamics in dielectrics. Before presenting our overview and findings, we provide a brief introduction of the tools and techniques used in this type of research.

2. Attosecond light pulses

In order to perform optical time-resolved spectroscopy with attosecond resolution, one needs to generate attosecond light pulses. This is done starting from an amplified femtosecond pulse in the infrared. In the most common implementation, this pulse is focused into a rare-gas jet inside a vacuum chamber. With a focused laser peak intensity on the order of 10^{14} W/cm^2, the electric field component of the electromagnetic wave forming the infrared pulse reaches a peak field strength that becomes comparable to the inner-atomic binding forces. As a result, the laser can strong-field ion-

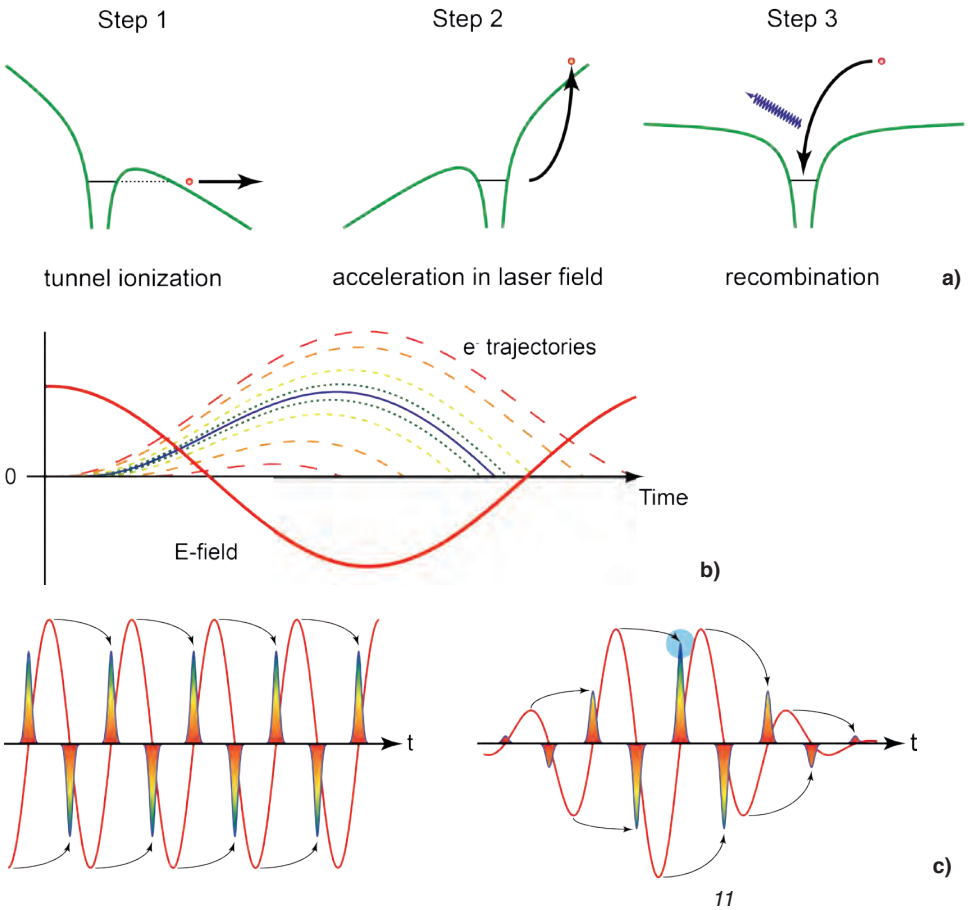

Figure 1: Attosecond pulse generation.
a) Three-step model of high-harmonic generation. The laser field tunnel-ionizes an atom by deforming its Coulomb potential (green lines). The liberated electron is then accelerated in the electric field of the laser pulse and with a certain probability recombines with the parent ion. Excess energy is emitted as a high-energy photon upon recombination.
b) Classical electron trajectories in oscillating laser field (solid red line). Only trajectories emerging within a quarter-cycle with decreasing amplitude return the parent ion (positioned on the horizontal axis). The color code of the trajectories encodes recollision energies (blue: high energy, red: low energy).
c) The process illustrated in a) and b) repeats for each half-cycle of the oscillating electric field. The arrows indicate the attosecond pulses that are emitted by recombination of electrons ionized around their origin. For a few-cycle pulse (right), the highest photon energies (marked by blue circle) are only generated for the electrons accelerated by the strongest half-cycle. High-pass filtering can therefore suppress all other attosecond pulses generated within this pulse.

ize the atoms. The liberated electrons are still exposed to the oscillatory electric field of the optical pulse. As the electric-field vector changes its direction with the optical oscillation, the electron can be accelerated back towards its parent ion, where it may recombine with a certain probability. Upon recombination, the excess energy gained by the electron during the acceleration cycle is emitted as a high-energy photon. This entire three-step process is known as high-order harmonic generation (HHG), which is also schematically illustrated in Figure 1a) [3-6]. For a pulse consisting of many field oscillation cycles, the process repeats for each sufficiently intense oscillation-half-cycle. As a consequence of this periodicity, the emitted radiation is found only at odd-order multiples of the initial infrared frequency. These harmonics can reach to very high orders due to the non-perturbative nature of this mechanism. A near-infrared driving laser centered at a wavelength of 800 nm (1.55 eV photon energy) will easily produce HHG radiation up to 80 eV (16 nm wavelength) or more. At first sight counterintuitively, a longer-wavelength driving laser can produce even higher energy photons at similar peak intensity, with record results reaching well beyond 1 keV [7]. The reason for this lies in the longer acceleration phase an electron experiences in a more slowly oscillating field.

The high-harmonic radiation is emitted in a coherent laser-like beam. The temporal structure of the emitted light is intrinsically attosecond. This can be intuitively understood when looking at the classical electron trajectories in the oscillating laser field. Only trajectories emerging during the falling quarter-cycle will actually return to the parent ion (Fig. 1b). Trajectories starting at other instances lead away from the ion. At 800 nm a full field oscillation cycle lasts 2.7 fs. A confinement of the emission to a quarter-cycle therefore already results in a sub-femtosecond pulse. The exponential field-strength dependence of the ionization probability leads to a further temporal confinement [8]. The shortest pulses to date have been measured at ETH Zürich and had a duration of 43 as [9].

If the driving infrared pulse consists of many comparably intense oscillation cycles, then a burst of attosecond pulses with half-infrared-cycle periodicity is generated. This burst is referred to as an attosecond pulse train (APT) [2] (Fig. 1c). If the HHG process is driven by a few-cycle pulse, however, the highest photon energies are produced only during the most intense half-cycle. With appropriate high-pass filtering and control of the relative phase between pulse envelope and carrier wave [10], a single attosecond pulse can be isolated [1] (Fig. 1c). An isolated attosecond pulse (IAP) has a continuous spectral power density, whereas an APT is formed by discrete harmonic peaks in the spectral domain. Both regimes are used in attosecond experiments.

3. Attosecond spectroscopy

The next ingredient to an attosecond experiment is a measurement technique that can exploit the short pulses generated through the above process to yield the desired temporal resolution. For their temporal resolution, ultrafast spectroscopic techniques typically rely on at least a pair of ultrashort optical pulses. One pulse (the so-called ‘pump’) initiates the dynamics one wants to measure, while a second pulse (the ‘probe’) probes the evolving system as a function of relative delay between the two pulses. For the probe pulse to be able to interrogate the dynamics started by the pump, the two pulses need to couple through an optical nonlinearity. In linear optics, the two pulses would just superimpose with no way for the probe to time-gate the response to the pump.

The need for an optical nonlinearity represents a particular challenge at the extreme ultraviolet (XUV) photon energies of the attosecond pulses. In general, optical nonlinearities are found to be small in that region of the electromagnetic spectrum compared to the visible or infrared domain. At the same time, the intensity of the attosecond pulses is comparably low because of the inefficient HHG process. As a consequence, most attosecond experiments rely on a two-color configuration where one of the two pulses is an intense infrared pulse with femtosecond duration while the other is the rather weak attosecond pulse. Which of the two assumes the role of the pump and which one is the probe depends on the specific experiment.

Attosecond spectroscopic techniques either record electron or optical spectra. In the former case, the energetic XUV photons of the attosecond pulse ionize a target. The resulting photoelectrons interact with the intense infrared probe. In the attosecond streak camera, the photoelectrons are accelerated or decelerated by the electric field of the infrared [1]. The final electron energy depends on the timing of the ionization event with respect to the probe. Compared to the field-free case, the electron energy is shifted up or down by the vector potential of the infrared pulse at the time of ionization (Fig. 2a). The electron spectra measured as a function of pump-probe delay correspond to the cross-correlation of the electron wavepacket created by the XUV pulse and the infrared vector potential. If transition matrix elements can be considered constant across the XUV spectrum, the electron wavepacket is essentially an energy-shifted replica of the XUV pulse. The attosecond resolution is maintained in this experiment despite the femtosecond duration of the probe because the measurement process is sensitive to the infrared field oscillations that show considerable variation on sub-femtosecond scales.

Using the same setup of the attosecond streak camera with attosecond pulse trains leads to a somewhat different result. If the infrared probe is derived from the same laser driving the HHG process, then the APT is formed by harmonics separated by twice the infrared photon energy (because only odd-order harmonics are generated). Photoelectrons created by the APT adopt its energetic structure. When interacting with the infrared probe, the photoelectrons created from a given harmonic can now absorb or emit an additional infrared photon. This brings the electron energy right in the middle between two adjacent harmonics. Because this final energy can be reached through the lower harmonic and absorption of an infrared photon as well as through the higher harmonic and emission of an infrared photon, interference between these two quantum mechanical pathways will occur (Fig. 2b). The interference on these so-called sidebands between the original harmonics modulates as a function of pump-probe delay. This method is referred to as reconstruction of attosecond beating by interference of two-photon transitions (RABBITT, [2, 11]).

How does one use the attosecond streak camera or RABBITT to resolve, for example, the attosecond dynamics of ionization processes? We can do so by performing measurements on either different ionization pathways of the same

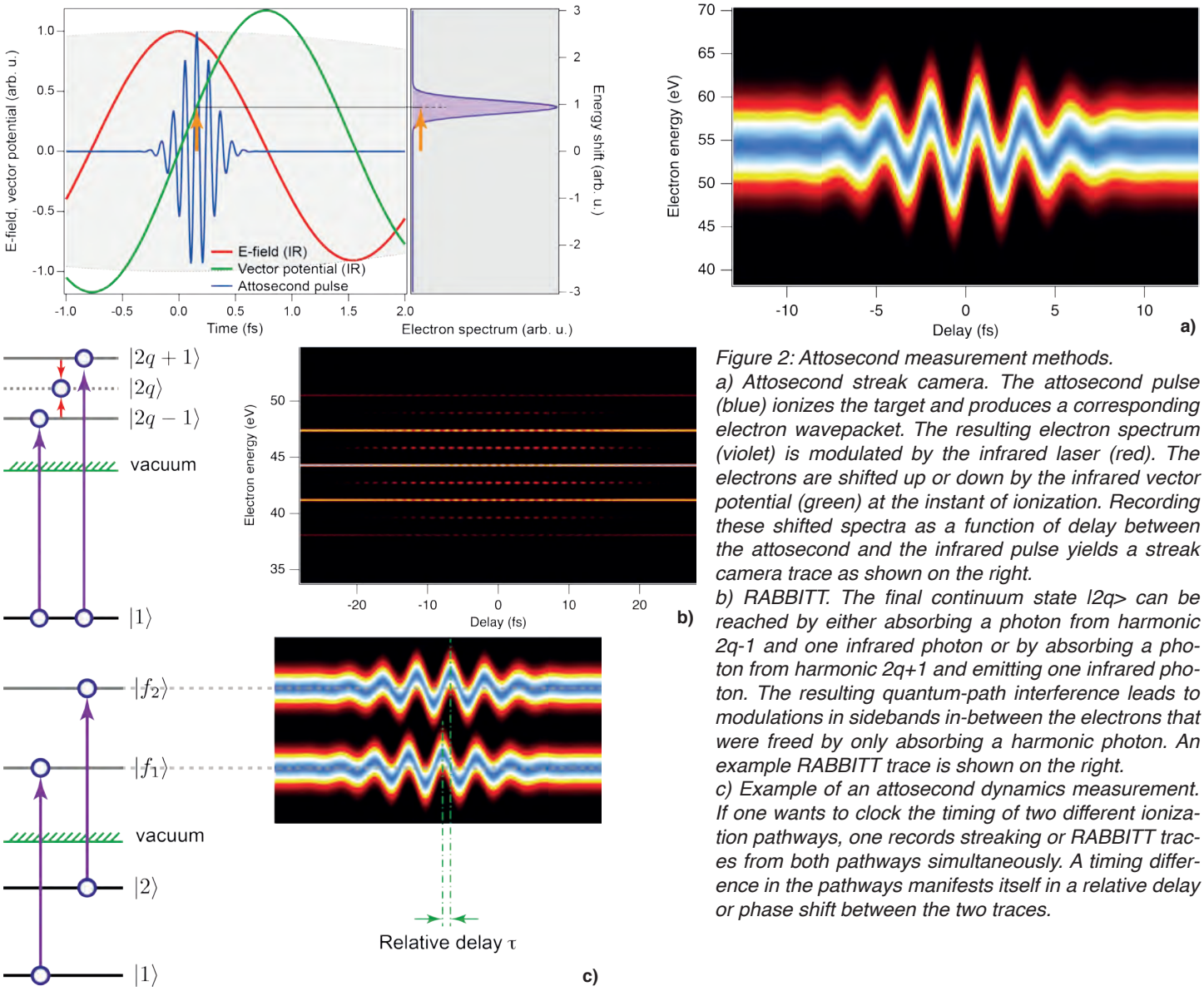

Figure 2: Attosecond measurement methods.
a) Attosecond streak camera. The attosecond pulse (blue) ionizes the target and produces a corresponding electron wavepacket. The resulting electron spectrum (violet) is modulated by the infrared laser (red). The electrons are shifted up or down by the infrared vector potential (green) at the instant of ionization. Recording these shifted spectra as a function of delay between the attosecond and the infrared pulse yields a streak camera trace as shown on the right.
b) RABBITT. The final continuum state |2q> can be reached by either absorbing a photon from harmonic 2q-1 and one infrared photon or by absorbing a photon from harmonic 2q+1 and emitting one infrared photon. The resulting quantum-path interference leads to modulations in sidebands in-between the electrons that were freed by only absorbing a harmonic photon. An example RABBITT trace is shown on the right.
c) Example of an attosecond dynamics measurement. If one wants to clock the timing of two different ionization pathways, one records streaking or RABBITT traces from both pathways simultaneously. A timing difference in the pathways manifests itself in a relative delay or phase shift between the two traces.

system (e.g. from two different initial states) or on different systems (e.g. ionization from the ground state of two different atomic species). If ionization happens more slowly in one case than in the other, the respective timing difference will manifest itself as a delay or phase shift between the data sets from the two pathways or systems (Fig. 2c). If the measurement is taken against a known reference, then the absolute timing of the ionization dynamics can be extracted [12]. A known reference can be a simple atomic system for which the ionization dynamics can be obtained with reasonable accuracy from theory. A more detailed analysis shows that the attosecond streak camera and RABBITT data provide within sampling constraints the full energy-dependent phase of the electron wavepacket created in the ionization event. This phase encodes the dynamics of the process.

Another important spectroscopic technique besides the electron-detecting streak camera and RABBITT is the all-optical attosecond transient absorption spectroscopy (ATAS, [13-15]). In this case, the infrared beam serves as a pump and initiates electron dynamics. The attosecond pulse probes these dynamics through resulting changes in the optical properties of the samples: either an increase or decrease of optical absorption. For this purpose, the optical spectrum of the transmitted attosecond pulse is recorded with and without the presence of the pump and as a function of pump-probe delay. The measurement in the absence of the pump yields the static reference for the optical properties of the sample if the process being studied has not been initiated. Any change in probe transmission observed when the pump is present must then be due to the induced dynamics. The actual dynamics is then observed by monitoring how the induced absorption change evolves as a function of pump-probe delay. If, for example, the pumped process transfers population that fills the final state of the probe transition, one would observe an increased probe transmission as fewer vacancies remain that can be populated by the probe. As the transferred population decays, vacancies become available again at sufficiently large delay of the probe to the pump. Transient absorption spectroscopy is a classical, well-established technique in the femtosecond domain and has been transferred to attosecond experiments around 2010 [13-15].

It should be noted that attosecond spectroscopic techniques can measure either electron or photon spectra with high energy resolution while maintaining attosecond pump-probe delay steps. An often found misconception is that this simultaneous high resolution in delay and energy is in conflict with the time-energy uncertainty. It is important to realize that we measure the spectra with a time-integrating detector as a function of relative delay between the pump and probe pulses rather than as a function of real time. A single de-

lay scan is therefore composed of individual measurements from many separate laser shots. Delay and energy are not conjugate quantities and therefore no uncertainty limitation applies in this case. The energy uncertainty arising from the short time duration of the involved pulses manifests itself, however, in their broad spectral bandwidth and the resulting low spectroscopic selectivity for addressing, for example, energetically closely spaced states with the pump pulse.

4. Attosecond photoemission spectroscopy of solids

The first attosecond experiments on solids were using the attosecond streak camera and later also RABBITT to resolve the photoemission dynamics from solid surfaces [16, 17]. The first streak camera experiments measured the timing between electrons photoemitted from the conduction band of a W(110) crystal with respect to electrons from the localized tungsten 4f core states [16]. RABBITT experiments on Au(111), Ag(111) and Cu(111) added energy resolution to the timing information and provided absolute delays calibrated against photoemission from argon atoms, which can be reasonably well calculated from theory [17, 18]. While the delays observed in previous experiments were consistent with assuming that the photoemission dynamics is dominated by ballistic transport of quasi-free electrons over an inelastic mean-free path to the surface, the RABBITT experiments revealed evidence for band-structure effects in the observed energy-dependence of the delays [18].

While our understanding of photoemission dynamics from solid surfaces is improving rapidly, many important questions remain open. Presently, the dynamics is interpreted in a three-step process that consists of excitation, transport to the surface and emission into the vacuum. This three-step model of photoemission is, of course, only an approximation of a true quantum mechanical description and it is known to fail under certain circumstances. With one notable exception [19], the experiments performed so far could satisfactorily be explained considering only the transport part of the three-step model. When do the other two steps need to be included and when does this three-step picture of photoemission fail altogether to properly describe the dynamics?

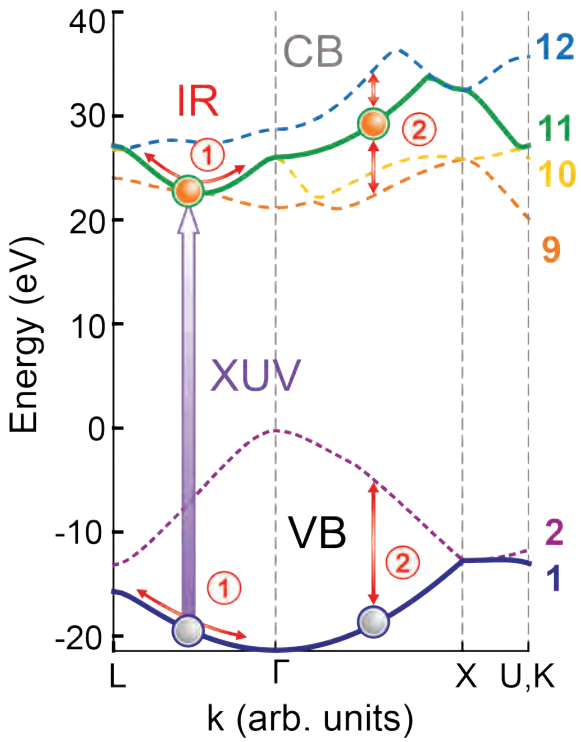

Figure 3: Intra- and inter-band dynamics. The illustration shows few selected sub-bands of the bandstructure of diamond. The horizontal red arrows represent infrared field driven intra-band electron motion (1) while the vertical arrows indicate inter-(sub-)band transitions induced by the infrared (2). The violet arrow shows the probe transition used in the ATAS experiment. The numbers on the right label individual sub-bands. The intermediate sub-bands 3-8 are not shown. (Figure reproduced from [21])

Both, attosecond streak camera as well as RABBITT, use a relatively intense infrared pulse to probe the dynamics. Past experiments show no evidence for the electron dynamics in the crystal to be modified through interaction with the infrared beam. This is not expected to hold universally. In particular for non-metallic samples, the infrared will deeply penetrate the crystal and expose the electrons to high light intensities already in the bulk. How does this infrared field interact with the crystal and its electronic structure? Can we still use the macroscopic laws of optics to describe experiments that probe dynamics on atomic spatial and temporal scales? While the Fresnel laws of optics that describe the reflection and transmission of optical waves at an interface were found to still hold on these scales for noble metals [20], it is an open question how well this finding transfers to other material classes.

5. Attosecond transient absorption spectroscopy of solids

The attosecond streak camera and RABBITT measure photoelectrons that are emitted from within few atomic layers from the solid-vacuum interface. As such, these methods are intrinsically surface sensitive. The optical absorption measured with attosecond transient absorption spectroscopy (ATAS), on the other hand, happens in the bulk of a material. ATAS therefore complements the above attosecond tool set for solid samples. While we covered the electron spectroscopy only briefly, we will give a more detailed view on ATAS and its application to different classes of solids.

As described in Section 3, in ATAS the infrared pulse assumes the role of the pump while the attosecond XUV pulse probes the induced absorption modifications. In the case of a solid, the pump serves as an external electric field that oscillates at optical frequencies and thus rapidly drives the electrons in the bulk. A question that immediately arises is whether the transient response, i.e., the direct sub-femtosecond to few-femtosecond reaction of the electronic system, is dominated by electrons being driven within their bands or by induced transitions to other bands (Fig. 3). We will address this question with experiments on two different material classes that differ strongly in their bandgap, leading to non-resonant and resonant excitation by the infrared pump, respectively.

For the large-bandgap, non-resonant case, we performed ATAS on 50-nm thick polycrystalline diamond films [21]. The thickness of the sample is dictated by the short absorption length of the attosecond XUV radiation in this material. A schematic of the used setup is shown in Figure 4a). The gas jet is used for performing a simultaneous attosecond streak camera measurement on Neon atoms. The streaking data serves as a reference to determine the exact timing

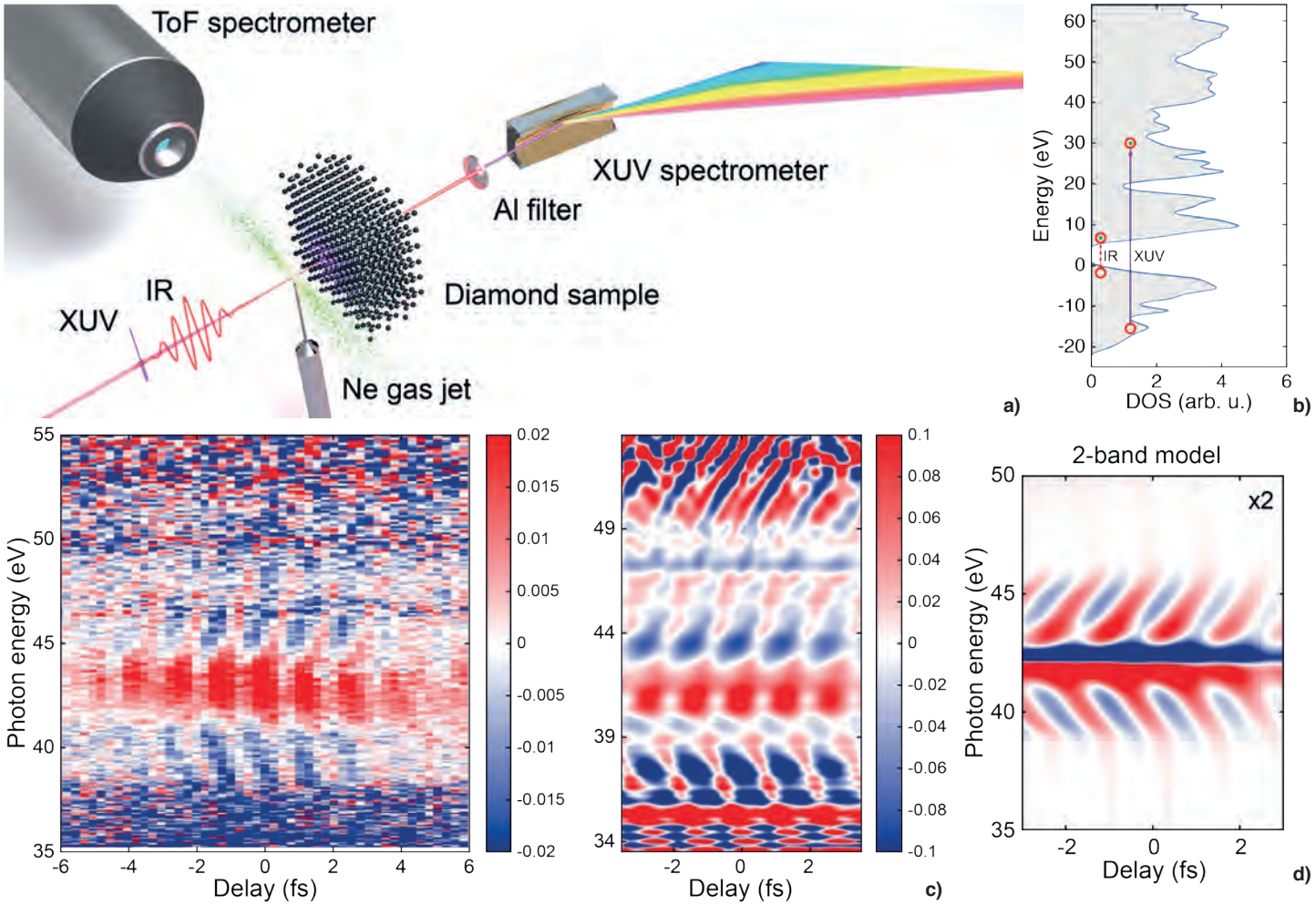

Figure 4: Attosecond transient absorption experiment in diamond. a) Experimental configuration. The Ne gas jet and the electron time-of-flight spectrometer are used to characterize the pump and probe pulses and provide the delay reference. b) While multi-photon absorption of the infrared pump can excite carriers into the conduction band, they are energetically well separated from the density-of-states probed by the attosecond XUV pulse. c) Transient absorption data (color scale indicates change in absorbance) from experiment (left) and ab initio theory (right). d) Even a very simple analytical two-band model captures the observed 'V'-shaped dispersion in the induced absorbance modulations. (Figures adapted from [21])

between the pump and the probe pulse. A simplified band diagram with the involved sub-bands is shown in Figure 3. It shows that the probe transition is from the bottom of the valence band high into the conduction band. The infrared pump photon energy is not enough to excite electrons from the valence to the conduction band. However, multi-photon transitions from the top of the valence band to the bottom of the conduction band may occur due to the relatively high infrared intensity (~10^{12} W/cm^2). Given that they are energetically well separated from the probe transition, they do not affect the measured ATAS signal (Fig. 4b).

The striking feature in the measured ATAS data are rapid oscillations of the absorption at twice the frequency of the infrared pump light. At the same time, the oscillations exhibit a 'V'-shaped dispersion with the apex of the 'V' lying at about 43 eV. To understand the observations, we performed time-dependent density functional theory. These *ab initio* calculations reproduce the qualitative signature of the measured signal well (Fig. 4c). Through an orbital decomposition and systematic elimination of unimportant sub-bands we were able to reduce the theory to only two dominating sub-bands (Fig. 4d) while maintaining the main features of the ATAS trace. Given that we only have two sub-bands left and considering the energetics, it follows that the infrared pump pulse can only drive electron motion within those bands while the attosecond pulse probes this dynamics through a transition between the two remaining bands. From this we conclude that the transient response of our diamond sample to an infrared optical field is dominated by intra-band motion rather than inter-band transitions. The observed signatures can be explained through the dynamical Franz-Keldysh effect which was previously observed with terahertz pump and optical probe pulses [21-23].

Considering the large bandgap of diamond, our findings might not be that surprising. How does the situation change if we replace the diamond sample with a 100-nm-thick crystalline GaAs membrane [24]? GaAs has a direct band gap (~1.42 eV) that is sufficiently small for a single infrared pump photon ($E_{ph} \approx 1.55$ eV) to promote electrons from the valence to the conduction band. Given that we kept the infrared intensity about the same as in the diamond experiment, one would intuitively expect that such single-photon transitions dominate the response of the material by far. In GaAs, the large bandwidth of the attosecond XUV pulse allowed probing the top of the valence band and the bottom of the conduction band simultaneously with a transition originating from the atomic As *3d* level.

The ATAS data measured in GaAs are shown in Figure 5a). The induced absorption shows again rapid modulations at twice the infrared frequency. An important difference com-

pared to the diamond case is that the induced absorption now has a lasting tail towards positive delays. This is due to the fact that the infrared can now transfer real population in the probed energy region, which was not possible for diamond. This population thermalizes and decays again on time scales much longer than the few femtoseconds being probed here. Again we first simulate the system with time-dependent density functional theory and then try to capture the main features of the conduction band dynamics with a simplified model. In the case of GaAs, a three-band model reproduces the observed features reasonably well. In this model, the probe transition occurs from the energetically lowest band to the highest band and the pump drives transitions between the mid-energy band and the highest band. The model thus includes the As *3d* state, a valence band and a conduction band.

In this simplified model, we can selectively switch intra-band and inter-band processes on and off (Fig. 5b). By definition, only inter-band transitions can create a lasting population of real carriers in the conduction band. Rather counterintuitively, however, it is found that the transient response of the sample (i.e. the few-femtosecond overlap region of the pump and probe pulses) is still dominated by intra-band dynamics despite the infrared pump pulse now driving the valence-to-conduction-band transition resonantly. A further inspection of the model also reveals that while intra-band electron motion alone cannot inject carriers into the conduction band, the coupling of intra-band motion and inter-band transitions leads to a three-fold enhancement of the number of injected carriers compared to a situation with inter-band dynamics only (Fig. 5c) [24]. The combination of our experimental data with a comparably simple theoretical model therefore gives important insights into carrier-injection mechanisms in optically pumped semiconductors.

These examples demonstrate how attosecond science can directly reveal optical-field-driven electron dynamics in solids that were inaccessible with previous methods. Given that the optical fields oscillate at hundreds of THz, these tools yield information that is relevant for the frequency scaling of electronic and opto-electronic components and provide hints about potential fundamental speed limitations of future devices. From a fundamental physics point of view, these experiments help to refine our understanding of light-matter interaction in solids on atomic spatial and temporal scales.

6. Conclusion and outlook

The attosecond science of solids is still a rather young research field. Most studies so far have concentrated on relatively simple materials and mainly focused on general fundamental mechanisms of light-matter interaction. As the experimental and theoretical tools mature, it is expected that the field will expand towards more complex material classes. At the same time, a wide range of potentially fast electronic processes, such as charge transfer at interfaces of different materials, still awaits investigation with these new tools. Higher pulse repetition rates of attosecond sources will improve the signal-to-noise ratio [25] and will be based

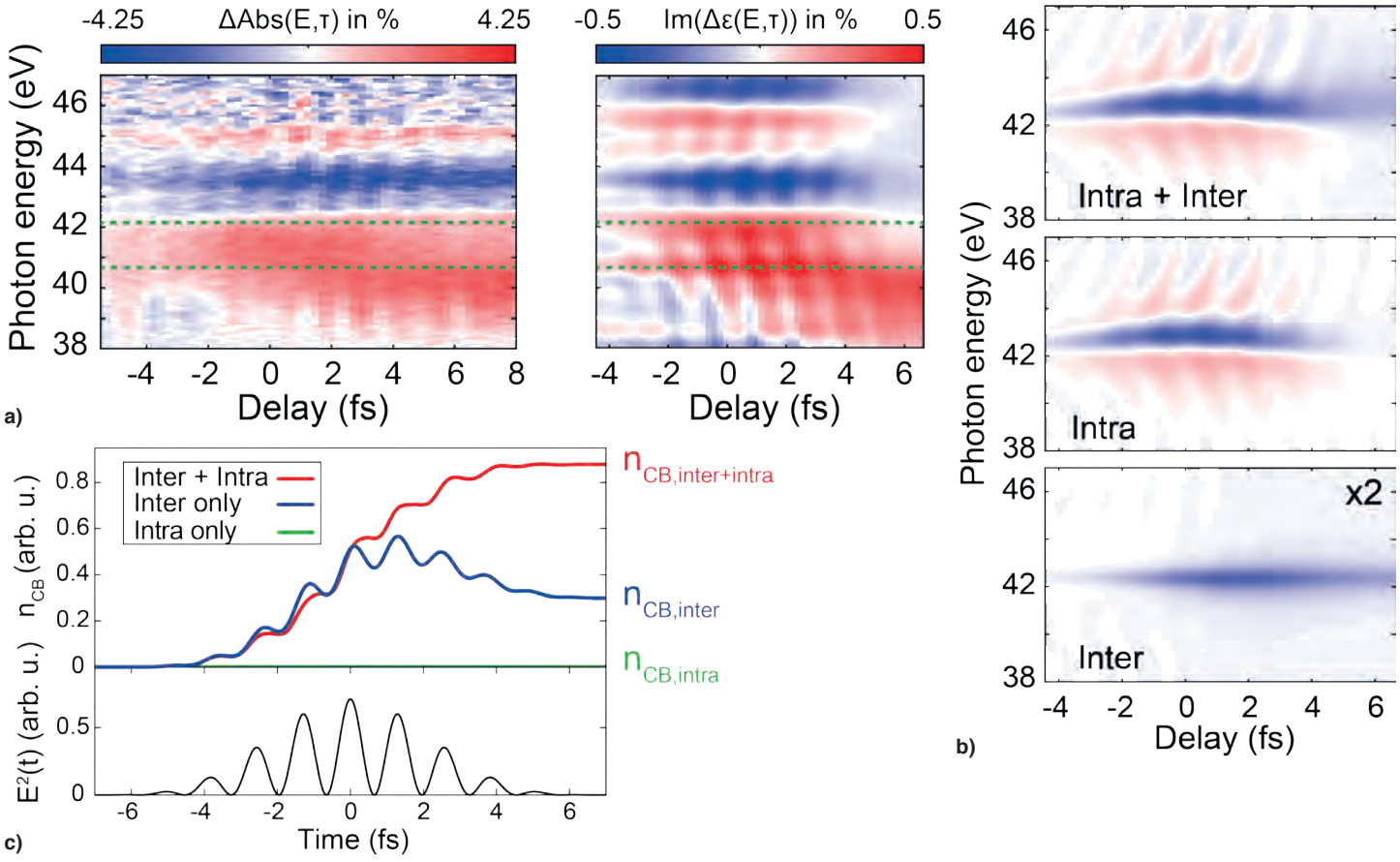

Figure 5: Attosecond transient absorption in GaAs. a) Transient absorption data (experiment, left; ab initio theory, right). The dashed green lines indicate the approximate positions of the field-free top of the valence band and bottom of the conduction band. b) Simulation of conduction band response with simple three-band model. The model indicates that the dominant features in the few-femtosecond transient response are due to intra-band electron dynamics. c) Number of carriers injected into the conduction band (top panel) and squared electric field of the infrared pump pulse (bottom panel). The coupling of intra- and inter-band dynamics results in a three-fold enhancement of the total of injected carriers. (Figures adapted from [24])

on average-power scaling of diode-pumped fiber [26], thin-disk [27] and slab [28] laser systems.

Meanwhile, with the European Extreme Light Infrastructure (ELI, [29]) becoming operational, attosecond sources will for the first time become accessible through a large user facility. Also the future ATHOS soft-X-ray beamline of SwissFEL at PSI is planned to provide an attosecond pulse mode to its users [30]. These pulses will be at photon energies that are difficult to reach with HHG and at a photon flux that is well beyond what is possible with conventional attosecond sources. Both of these developments will help to expand the community towards groups that are not specialists in the generation and handling of attosecond pulses. Through coverage of new parameter ranges, these facilities will enable entire new classes of experiments. It is expected that the few examples discussed in this article are therefore merely a beginning of the attosecond science of solids and beyond.

References

[1] M. Hentschel, R. Kienberger, C. Spielmann, G. A. Reider, N. Milosevic, T. Brabec, P. Corkum, U. Heinzmann, M. Drescher, and F. Krausz, "Attosecond metrology," Nature **414**, 509-513 (2001).

[2] P. M. Paul, E. S. Toma, P. Breger, G. Mullot, F. Augé, P. Balcou, H. G. Muller, and P. Agostini, "Observation of a Train of Attosecond Pulses from High Harmonic Generation," Science **292**, 1689-1692 (2001).

[3] M. Ferray, A. L'Huillier, X. F. Li, L. A. Lompré, G. Mainfray, and C. Manus, "Multiple-harmonic conversion of 1064 nm radiation in rare gases," J. Phys. B: At. Mol. Opt. Phys. **21**, L31-L35 (1988).

[4] X. F. Li, A. L'Huillier, M. Ferray, L. A. Lompre, and G. Mainfray, "Multiple-harmonic generation in rare gases at high laser intensity," Phys. Rev. A **39**, 5751-5761 (1989).

[5] A. McPherson, G. Gibson, H. Jara, U. Johann, T. S. Luk, I. A. McIntyre, K. Boyer, and C. K. Rhodes, "Studies of multiphoton production of vacuum-ultraviolet radiation in the rare gases," J. Opt. Soc. Am. B **4**, 595-601 (1987).

[6] P. B. Corkum, "Plasma Perspective on Strong-Field Multiphoton Ionization," Phys. Rev. Lett. **71**, 1994-1997 (1993).

[7] T. Popmintchev, M.-C. Chen, D. Popmintchev, P. Arpin, S. Brown, S. Ališauskas, G. Andriukaitis, T. Balčiunas, O. D. Mücke, A. Pugzlys, A. Baltuška, B. Shim, S. E. Schrauth, A. Gaeta, C. Hernández-García, L. Plaja, A. Becker, A. Jaron-Becker, M. M. Murnane, and H. C. Kapteyn, "Bright Coherent Ultrahigh Harmonics in the keV X-ray Regime from Mid-Infrared Femtosecond Lasers," Science **336**, 1287-1291 (2012).

[8] M. V. Ammosov, N. B. Delone, and V. P. Krainov, "Tunnel ionization of complex atoms and of atomic ions in an alternating electromagnetic field," Sov. Phys. JETP **64**, 1191-1194 (1986).

[9] T. Gaumnitz, A. Jain, Y. Pertot, M. Huppert, I. Jordan, F. Ardana-Lamas, and H. J. Wörner, "Streaking of 43-attosecond soft-X-ray pulses generated by a passively CEP-stable mid-infrared driver," Opt. Express **25**, 27506 (2017).

[10] H. R. Telle, G. Steinmeyer, A. E. Dunlop, J. Stenger, D. H. Sutter, and U. Keller, "Carrier-envelope offset phase control: A novel concept for absolute optical frequency measurement and ultrashort pulse generation," Appl. Phys. B **69**, 327-332 (1999).

[11] H. G. Muller, "Reconstruction of attosecond harmonic beating by interference of two-photon transitions," Appl. Phys. B **74**, S17-S21 (2002).

[12] R. Locher, M. Lucchini, J. Herrmann, M. Sabbar, M. Weger, L. A., L. Castiglioni, M. Greif, M. Hengsberger, L. Gallmann, and U. Keller, "Versatile attosecond beamline in a two-foci configuration for simultaneous time-resolved measurements," Rev. Sci. Instr. **85**, 013113 (2014).

[13] E. Goulielmakis, Z.-H. Loh, A. Wirth, R. Santra, N. Rohringer, V. S. Yakovlev, S. Zherebtsov, T. Pfeifer, A. M. Azzeer, M. F. Kling, S. R. Leone, and F. Krausz, "Real-time observation of valence electron motion," Nature **466**, 739-743 (2010).

[14] H. Wang, M. Chini, S. Chen, C.-H. Zhang, F. He, Y. Cheng, Y. Wu, U. Thumm, and Z. Chang, "Attosecond Time-Resolved Autoionization of Argon," Phys. Rev. Lett. **105**, 143002 (2010).

[15] M. Holler, F. Schapper, L. Gallmann, and U. Keller, "Attosecond Electron Wave-Packet Interference Observed by Transient Absorption," Phys. Rev. Lett. **106**, 123601 (2011).

[16] A. L. Cavalieri, N. Müller, T. Uphues, V. S. Yakovlev, A. Baltuska, B. Horvath, B. Schmidt, L. Blümel, R. Holzwarth, S. Hendel, M. Drescher, U. Kleineberg, P. M. Echenique, R. Kienberger, F. Krausz, and U. Heinzmann, "Attosecond spectroscopy in condensed matter," Nature **449**, 1029-1032 (2007).

[17] R. Locher, L. Castiglioni, M. Lucchini, M. Greif, L. Gallmann, J. Osterwalder, M. Hengsberger, and U. Keller, "Energy-dependent photoemission delays from noble metal surfaces by attosecond interferometry," Optica **2**, 405-410 (2015).

[18] L. Kasmi, M. Lucchini, L. Castiglioni, P. Kliuiev, J. Osterwalder, M. Hengsberger, L. Gallmann, P. Krüger, and U. Keller, "Effective mass effect in attosecond electron transport," Optica **4**, 1492-1497 (2017).

[19] F. Siek, S. Neb, P. Bartz, M. Hensen, C. Strüber, S. Fiechter, M. Torrent-Sucarrat, V. M. Silkin, E. E. Krasovskii, N. M. Kabachnik, S. Fritzsche, R. D. Muiño, P. M. Echenique, A. K. Kazansky, N. Müller, W. Pfeiffer, and U. Heinzmann, "Angular momentum–induced delays in solid-state photoemission enhanced by intra-atomic interactions," Science **357**, 1274-1277 (2017).

[20] M. Lucchini, L. Castiglioni, L. Kasmi, P. Kliuiev, A. Ludwig, M. Greif, J. Osterwalder, M. Hengsberger, L. Gallmann, and U. Keller, "Light-Matter Interaction at Surfaces in the Spatiotemporal Limit of Macroscopic Models," Phys. Rev. Lett. **115**, 137401 (2015).

[21] M. Lucchini, S. A. Sato, A. Ludwig, J. Herrmann, M. Volkov, L. Kasmi, Y. Shinahara, K. Yabana, L. Gallmann, and U. Keller, "Attosecond dynamical Franz-Keldysh effect in polycrystalline diamond," Science **353**, 916-919 (2016).

[22] K. B. Nordstrom, K. Johnsen, S. J. Allen, A.-P. Jauho, B. Birnir, J. Kono, T. Noda, H. Akiyama, and H. Sakaki, "Excitonic Dynamical Franz-Keldysh Effect," Phys. Rev. Lett. **81**, 457 (1998).

[23] F. Novelli, D. Fausti, F. Giusti, F. Parmigiani, and M. Hoffmann, "Mixed regime of light-matter interaction revealed by phase sensitive measurements of the dynamical Franz-Keldysh effect," Sci. Rep. **3**, 1227 (2013).

[24] F. Schlaepfer, M. Lucchini, S. A. Sato, M. Volkov, L. Kasmi, N. Hartmann, A. Rubio, L. Gallmann, and U. Keller, "Attosecond optical-field-enhanced carrier injection into the GaAs conduction band," Nat. Phys. **14**, 560-564 (2018).

[25] T. Südmeyer, S. V. Marchese, S. Hashimoto, C. R. E. Baer, G. Gingras, B. Witzel, and U. Keller, "Femtosecond laser oscillators for high-field science," Nature Photonics **2**, 599-604 (2008).

[26] M. Müller, M. Kienel, A. Klenke, T. Gottschall, E. Shestaev, M. Plötner, J. Limpert, and A. Tünnermann, "1 kW 1 mJ eight-channel ultrafast fiber laser," Optics Letters **41**, 3439-3442 (2016).

[27] C. J. Saraceno, F. Emaury, O. H. Heckl, C. R. E. Baer, M. Hoffmann, C. Schriber, M. Golling, T. Südmeyer, and U. Keller, "275 W average output power from a femtosecond thin disk oscillator operated in a vacuum environment," Opt. Express **20**, 23535-23541 (2012).

[28] P. Russbueldt, T. Mans, J. Weitenberg, H. D. Hoffmann, and R. Poprawe, "Compact diode-pumped 1.1 kW Yb:YAG Innoslab femtosecond amplifier," Opt. Lett. **34**, 4169-4171 (2010).

[29] "Extreme Light Infrastructure, The ELI Project," (ELI Delivery Consortium), *https://eli-laser.eu/the-eli-project/*.

[30] "SwissFEL," (Paul Scherrer Institut), *https://www.psi.ch/swissfel/*.